Journal of Power Sources 187 (2009) 268–274

Contents lists available at ScienceDirect

Journal of Power Sources

journal homepage: www.elsevier.com/locate/jpowsour

Effect of compounding process on the structure and electrochemical properties of ordered mesoporous carbon/polyaniline composites as electrodes for supercapacitors

Lixia Li, Huaihe Song*, Qincang Zhang, Jingyuan Yao, Xiaohong Chen

State Key Laboratory of Chemical Resource Engineering, Beijing University of Chemical Technology, 100029 Beijing, PR China

ARTICLE INFO

Article history:
Received 10 April 2008
Received in revised form
24 September 2008
Accepted 24 October 2008
Available online 31 October 2008

Keywords:
Polyaniline
OMC
Supercapacitor
In situ polymerization
Double fixing effects

ABSTRACT

Polyaniline (PANI) loaded ordered mesoporous carbon (OMC) composites were prepared via different processes, involving the in situ polymerization of aniline in the presence of OMC or its precursor and the direct physical mixing method. On the basis of analyzing the morphologies and structures of these three OMC/PANI composites, the influence of compounding processes on the electrochemical properties as electrodes for supercapacitors was first investigated. It was observed that regardless of compounding process, two distinct electrochemical behaviors took place on all of the composite electrodes, including a redox reaction with insertion and deinsertion of electrolyte ions, and electrostatic attraction at the electrode/electrolyte interface. Additionally, these OMC/PANI composites showed higher specific capacitances compared with pure OMC and PANI. Most significantly, the in situ synthesized OMC/PANI composite using OMC as a starting material exhibited the highest specific capacitance of 747 $F g^{-1}$ at a current density of 0.1 $A g^{-1}$ and excellent rate capability, which was attributed to the high degree of dispersion of PANI and the contact of PANI with electrolyte as well as the double fixing effects of surface and mesopore of OMC on PANI.

1. Introduction

As a novel kind of energy storage device, the supercapacitor with high energy and high power density has attracted growing attention owing to its wide range of potential applications in hybrid electric vehicles, fuel cells, cellular phones, PDAs, etc. [1]. According to the mechanism of energy storage, two types of supercapacitors are under development: one is the electric double-layer capacitor (EDLC), in which stored energy is accumulated by the separation of electronic and ionic charges at the interface between a high surface area electrode and an electrolyte solution; the other is the pseudocapacitor, in which the active species can be fast and reversibly oxidized and reduced at characteristic potentials.

Following the report of Ryoo et al. of CMK-1 in 1999 [2], ordered mesoporous carbons (OMCs) have been widely studied as the electrode materials for EDLCs considering their well-ordered pore channels, high specific surface areas, narrow pore size distributions [3–6]. It has been proved that these materials are especially adapted for high current densities. However, compared with conducting polymers or metal oxides (such as RuO_2) [7,8], the specific capacitances of OMCs are relatively low.

For pseudocapacitors, polyaniline (PANI) is a frequently used electrode material, not only owing to its high specific capacitance, but because of a lot of advantages for practical applications, such as cheapness of preparation, ease of polymerization in aqueous media, high stability in air, simplicity in doping/dedoping, etc. [9–11]. However, it is well known [12,13] that contrary to porous carbon the main drawback for PANI as supercapacitor electrode is the poor cycling stability derived from the big volumetric change in the doping/dedoping process. Therefore, the compounding of porous carbon and PANI seems to be an effective method to fully utilize their respective advantages.

The combination of PANI with various porous carbon materials has been proved to be attractive to reinforce the stability of PANI as well as maximize the capacitance value. For example, Chen and Wen [14] reported that the specific capacitance can be improved from 95 $F g^{-1}$ of pure-carbon electrode to 160 $F g^{-1}$ of PANI–carbon composite electrode by the electropolymerization on the surface of activated porous carbon. Jang et al. [15] studied a polyaniline-coated carbon nanofiber prepared by one-step vapor deposition polymerization technique. It was deduced that the specific capacitance of the composite was significantly dependent on

* Corresponding author. Tel.: +86 10 64434916; fax: +86 10 64434916.
E-mail address: songhh@mail.buct.edu.cn (H. Song).

0378-7753/$ – see front matter © 2008 Elsevier B.V. All rights reserved.
doi:10.1016/j.jpowsour.2008.10.075

the thickness of PANI layer and the value was as high as 264 F g^{-1} at the coating thickness of 20 nm. Furthermore, it was reported [16] that 73 wt.% PANI-deposited single-wall carbon nanotube electrode showed not only a high specific capacitance of 485 F g^{-1} but also an excellent cycling stability.

It is worth noting that the capacitive performance of the supercapacitor was once enhanced via the direct introduction of PANI to OMC [17]. It was reported in that study that the specific capacitance was as high as 900 F g^{-1} at a current density of 0.1 A g^{-1}. However, in view of the fact that the mesopores of OMC were filled by PANI molecules the specific surface area of the resultant composite was only 35 m^2 g^{-1} and thus the electric double-layer capacitance of OMC could not have been sufficiently utilized. Therefore, it is necessary to investigate in detail the influence of the compounding process between OMC and PANI on the capacitor performance of PANI/OMC composite. Herein two types of OMC/PANI composites were chemically synthesized by in situ polymerization of aniline in the presence of OMC and its precursor (carbon/silica composite). For comparison, a direct physical mixing method was also used to prepare the OMC/PANI composite. The morphology, pore structure and supercapacitor performance of the resultant composites were investigated, and the relationship between the interaction mechanism of OMC and PANI and electrochemical characteristics was further deduced.

2. Experimental

2.1. Synthesis of OMC and carbon/silica composite

Ordered mesoporous carbon was prepared as reported in the literature [18]. The typical process was performed as follows: (1) 5 g of triblock copolymer P123 (Aldrich) was dissolved in a solution composed of 130 mL of de-ionized water and 6.36 mL of concentrated sulfuric acid at 313 K. After stirring for 3 h, 9.2 mL of tetraethyl orthosilicate (TEOS, 98 wt.%) was added dropwise to the above solution with stirring. The resulting solution was aged at 313 K for 24 h, followed by further aging at 373 K for 36 h. The resultant precipitate was filtered, washed and dried at room temperature to obtain the as-synthesized composite; (2) the as-synthesized composite was dried in a drying oven at 373 K for 6 h and subsequently 433 K for another 6 h; (3) the resultant dark brown material was carbonized in a horizontal furnace under pure nitrogen atmosphere at 1123 K for 2 h for the complete carbonization of P123 and the carbon/silica composite was obtained; (4) the resultant carbon/silica composite was immersed in 48 wt.% hydrofluoric acid (HF) at room temperature for 24 h to remove the silica template; (5) the OMC material obtained as an insoluble fraction was repeatedly washed with de-ionized water and dried in air at 373 K.

2.2. Preparation of OMC/PANI composites

Composite 1: 2.55 g of OMC was immersed in a solution containing 2.5 mL of aniline, 5 mL of 6 mol L^{-1} hydrochloric acid (HCl) and 50 mL of water. After stirring for 30 min, an ammonium persulfate (APS) solution including 25 mL of water and 5.7 g of APS was added dropwise at 273 K and stirring continued for a further 3 h. The resulting product was filtered and washed repeatedly with acetone, HCl and de-ionized water, respectively. Finally the resulting composite was dried under vacuum at 373 K for 24 h. The 50 wt.% of mass load of PANI in the composite was evaluated by calculating the weight increase of OMC.

Composite 2: The overall synthetic procedure was similar to that of composite 1. The only difference was to use 8.5 g of carbon/silica composite (obtained in step 3 of Section 2.1) instead of 2.55 g of OMC as a starting material. After the polymerization the silica template was removed by using 48 wt.% HF. The mass load of PANI in the composite was also 50 wt.%.

Composite 3: This was obtained by a simple mixing of 2.55 g of OMC and 2.55 g of PANI. The PANI was synthesized using the same mass ratio of ANI:APS:HCl:H_2O mentioned above.

2.3. Characterization of OMC/PANI composites

The composite materials were characterized by X-ray diffraction (XRD), Fourier transform infrared spectroscope (FTIR), field emission scanning electron microscope (FE-SEM) and N_2 adsorption–desorption measurements. XRD patterns were recorded on a Rigaku D/max-2500B2 + /PCX system operating at 40 kV and 20 mA using Cu Kα radiation (λ = 1.5406 Å). FTIR spectra were recorded on a Nicolet 210 FTIR spectrometer. FE-SEM was conducted using JEOL JSM-6700 electron microscope at 10 kV. Nitrogen adsorption–desorption isotherms were performed with ASAP 2020 Micromeritics Instrument at 77 K. The pore size distributions were calculated by the BJH (Barrett–Joyner–Halenda) method from the desorption branch. The specific surface areas (S_{BET}) were calculated from the adsorption data in the relative pressure interval from 0.04 to 0.2 using the Brunauer–Emmett–Teller (BET) method. The total pore volumes (V) were estimated from the amount adsorbed at a relative pressure of 0.98.

2.4. Assembly and measurement of OMC/PANI composite electrodes

The supercapacitor electrodes were prepared by pressing a mixture of the resulting composite (78 wt.%), graphite (20 wt.%), and polytetrafluoroethylene (PTFE) (2 wt.%) to the graphite sheet that served as a current collector. The electrodes have a geometric surface area of 100 mm^2 and thickness of 0.4 mm. The mass load of the prepared electrode was 10 mg cm^{-2}. Platinum foil and Hg/HgO electrodes were used as the counter and reference electrodes, respectively. The electrolyte was 30 wt.% KOH aqueous solution. The electrochemical performances of the prepared electrodes were characterized by galvanostatic charge/discharge, cyclic voltammetry (CV) and AC impedance tests. The galvanostatic charge/discharge capacitance (C) was measured using a Program Testing System (produced by China-Land Com. Ltd., China). Charge and discharge voltages ranged between 0.9 and 0.01 V. The C in farad was calculated on the basis of [19]

$$C = \frac{I \times \Delta t}{\Delta V \times m} \quad (1)$$

where C is the specific capacitance, I the constant discharge current, Δt the discharge time, ΔV the voltage difference in discharge and m is the mass of active material within the electrode.

The cyclic voltammetry and AC impedance were carried out with a CHI 660B electrochemical working station. For the cyclic voltammetric measurements, the sweep rate ranged from 1 to 10 mV s^{-1} within a potential range of 0.05 to 0.55 V. For the AC impedance measurements, the potential amplitude of AC was kept as 10 mV and the frequency range was from 10 kHz to 1 mHz.

3. Results and discussion

The morphologies of the obtained pristine OMC, PANI and OMC/PANI composites were observed by FE-SEM and their images are shown in Fig. 1. As seen from Fig. 1A and B, the prepared mesoporous carbon and polyaniline are made of fasciculi and granular corals, respectively. Since composite 3 is a direct mixing product of OMC and PANI, both granular corals and fasciculi morphologies

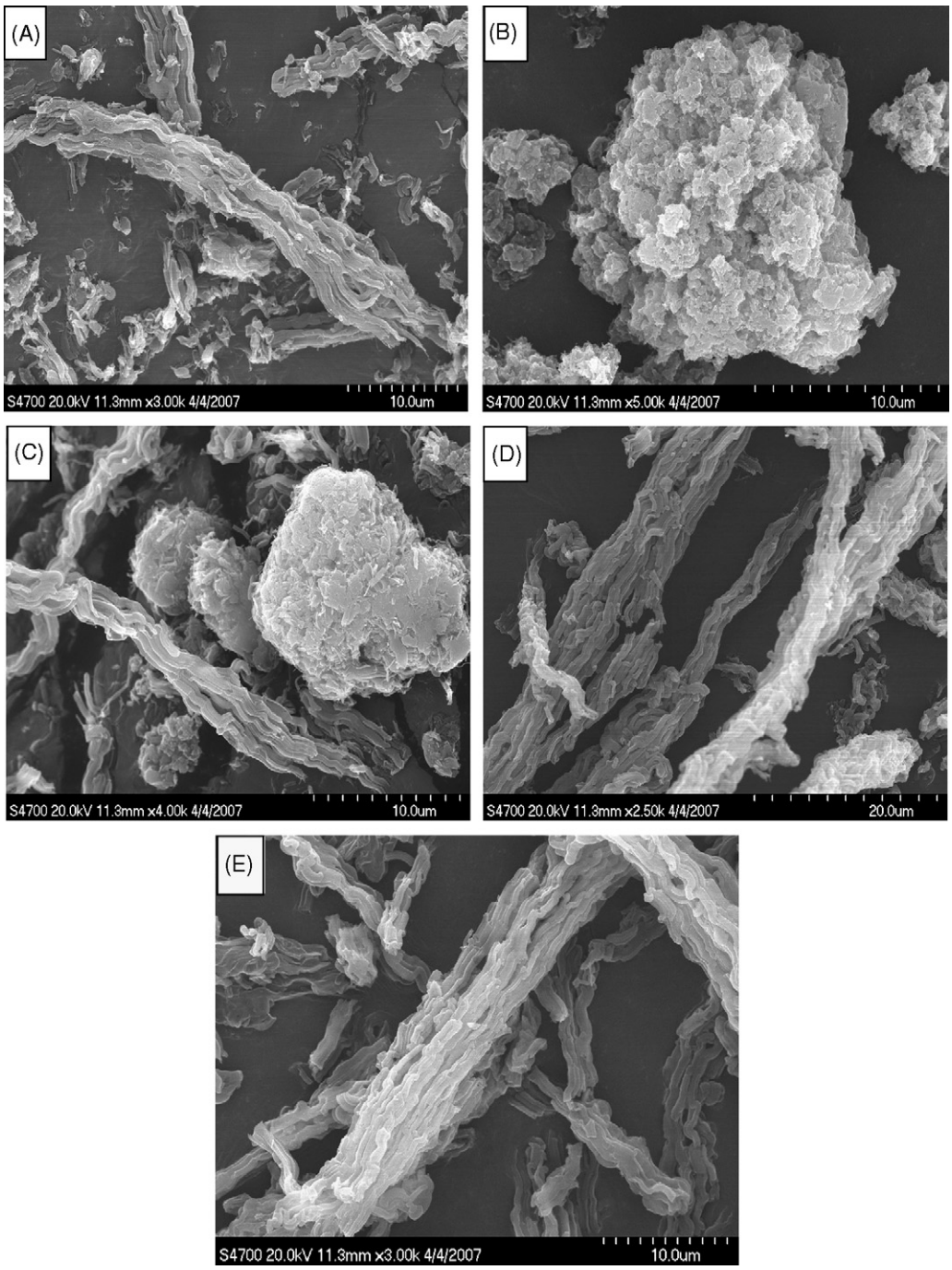

Fig. 1. FE-SEM images of OMC (A), PANI (B), composite 3 (C), composite 1 (D) and composite 2 (E).

are observed in Fig. 1C. On the other hand, the products prepared via in situ polymerization method, composite 1 and composite 2 (see Fig. 1D and E, respectively) exhibit only fasciculi with no granular corals, implying that the polymerization of aniline occurred either on the surface of the starting material or inside the pore. It also indicates that whatever starting material was used, either OMC or carbon/silica composite, the interactions between OMC and PANI exist in the chemically synthetic OMC/PANI composites, which would be beneficial to the improvement of both electric conductivity and further specific capacitance as discussed below.

In order to ascertain the origins of the interactions, FTIR, XRD and N_2 sorption measurements were used. FTIR spectra of pure OMC, PANI and OMC/PANI composites are shown in Fig. 2. A characteristic stretching vibration of C–O–C group [20] at 1096 cm^{-1} appears in FTIR spectrum 'a' of OMC, which would be an important active site for interactions of PANI and OMC in both composite 1 and composite 2. In the spectra of pure PANI (b) and composite 3 (c), the key characteristic peaks corresponding to the quinoid ring and the benzene ring are observed at 1562 and 1482 cm^{-1}, respectively. The other peaks at 1293, 1119 and 795 cm^{-1} can be assigned to the C—N stretching of the secondary aromatic amine, aromatic C—H in-plane bending and out-of plane C—H bending vibration, respectively. Based on the reported literatures [21,22], it can be deduced that HCl-doped PANI was obtained in our experiment. In addition,

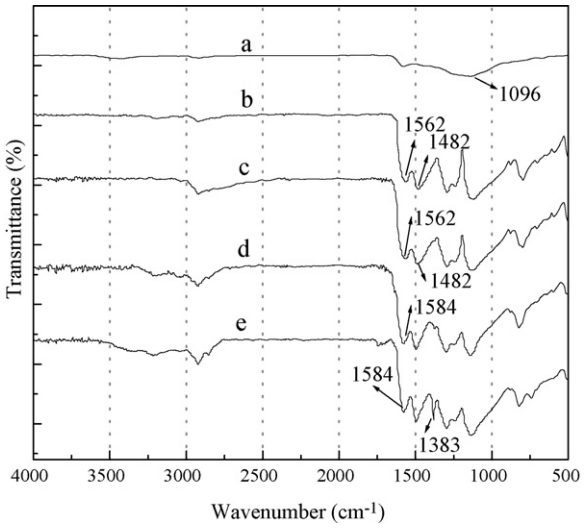

Fig. 2. FTIR spectra of OMC (a), PANI (b), composite 3 (c), composite 1 (d) and composite 2 (e).

for spectra 'd' and 'e' of composite 1 and composite 2 prepared via in situ polymerization method, all characteristic peaks show a shift to higher frequencies owing to the presence of interactions between PANI and OMC. Importantly, a new peak appears at 1383 cm^{-1} in composite 2, which resulted from the doping with HF [23].

Fig. 3a shows the N_2 adsorption–desorption isotherms of OMC and composite 2. It can be seen that their isotherms are similar to the shape of type IV [24], suggesting that both are mesoporous materials. Their corresponding pore size distribution curves derived from the BJH method are shown in Fig. 3b. The narrow pore size distributions centered at about 3.32 nm for OMC and 3.34 nm for composite 2 clearly demonstrate that during the preparation of composite 2 the removal of silica did not alter the mesopore structure of OMC. The BET surface areas and pore volumes of OMC and composite 2 were calculated to be about 844 and 307 $m^2\,g^{-1}$ and 0.90 and 0.34 $cm^3\,g^{-1}$, respectively. The lower values of composite 2 compared with pure OMC are mainly ascribed to the presence of dense polyaniline (the BET surface area of pure PANI measured by N_2 adsorption is 11 $m^2\,g^{-1}$). Theoretically, the BET surface area of composite 2 should be 420 $m^2\,g^{-1}$ by the simple sum based on the weight content (50:50) of OMC and PANI. However, since some aniline molecules are polymerized in the carbon channels of the carbon/silica composite, some pores of the starting material are occupied by PANI and thus the measured value is lower than the theoretical value. Furthermore, composite 1 exhibits much lower surface area of 86.5 $m^2\,g^{-1}$ compared with composite 2, implying that the main mesopores of OMC in composite 1 are blocked by PANI molecules.

Fig. 4 shows the XRD patterns of OMC, composite 1 and composite 2. It can be seen that both OMC (a) and composite 2 (b) exhibit a well-ordered periodic structure as indicated by the presence of low angle correlation peaks assigned to (1 0 0), (1 1 0) and (2 0 0) planes. However, these peaks are not found in the XRD pattern of composite 1 (c), suggesting that in composite 1 prepared using OMC as a starting material the ordered pore structure of OMC disappears, while in composite 2 prepared using the OMC precursor as a starting material most mesopores of OMC are retained. This is in good accordance with the results obtained from the BET surface areas. It is reasonable to believe that, for composite 1 PANI molecules are distributed not only on the surface but also partially in the pore of OMC, which increases both the degree of dispersion of PANI and the contact of PANI with electrolyte, and thus may

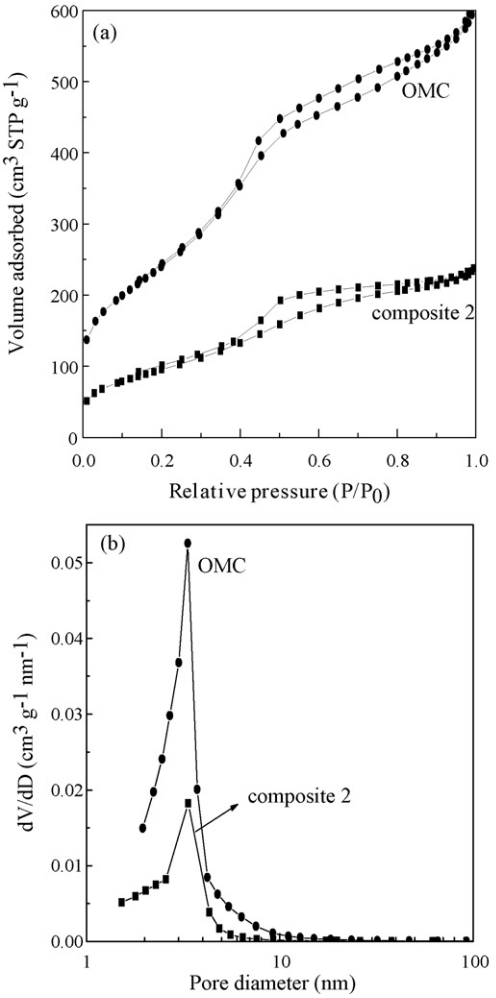

Fig. 3. N_2 adsorption–desorption isotherms (a) and pore size distributions (b) of OMC and composite 2.

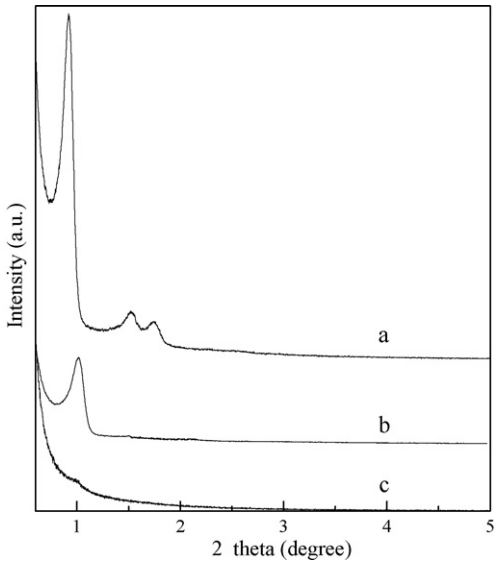

Fig. 4. XRD patterns of OMC (a), composite 2 (b) and composite 1 (c).

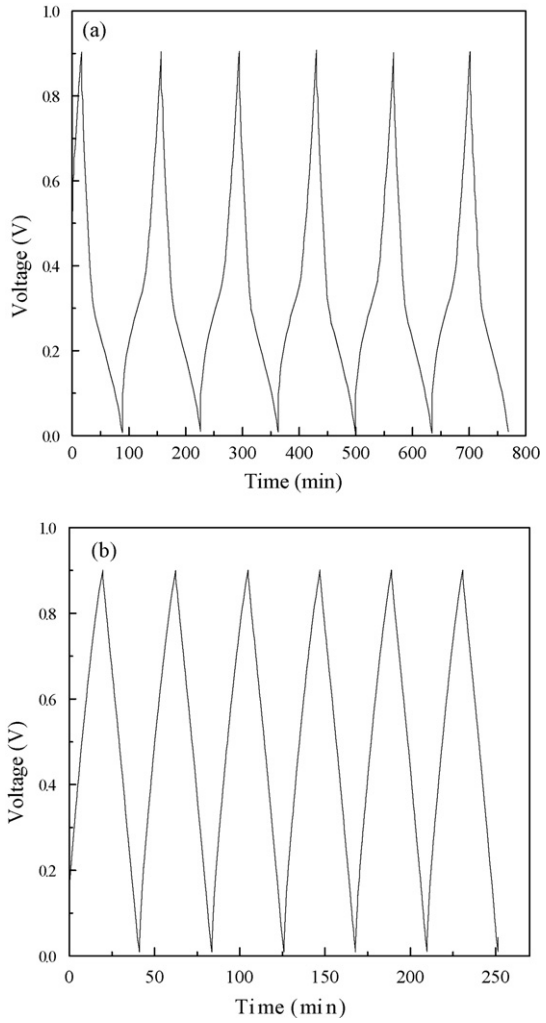

Fig. 5. Galvanostatic charge/discharge cycling curves of composite 1 (a) and OMC (b) at a current density of 0.1 A g^{-1}.

be favorable for the enhancement of the electrochemical performance as an electrode for supercapacitor. At the same time, OMC will provide a stronger support for PANI than in composite 2, which will ultimately favor maintaining the electrical conductivity [21,25] and mechanical strength [26] of PANI and thus the supercapacitor performance will be improved as well.

To investigate the electrochemical performance of the resulting composites as electrodes for supercapacitors, galvanostatic charge/discharge cycling measurements were performed. The result of composite 1 measured at a current density of 0.1 A g^{-1} is shown in Fig. 5a. For the purpose of comparison, the cycle property of the OMC electrode was also tested and the result is shown in Fig. 5b. From the typical triangular-shaped curve it is apparent that the OMC electrode exhibits an ideal double-layer capacitor behavior. The curve shape of composite 1 electrode, however, is different from that of OMC electrode, that is, two clear voltage stages are included: 0.9–0.35 and 0.35–0.01 V, respectively. During the former, short charge/discharge duration is shown, which is ascribed purely to the electric double-layer capacitance of the electrode. The latter is different. Since faradaic charge-transfer is usually accompanied by the double-layer charging process [27], the combination of electric double-layer capacitance and faradaic capacitance is responsible for the longer charge/discharge duration. Similar patterns are also observed for composite 2 and composite 3 electrodes.

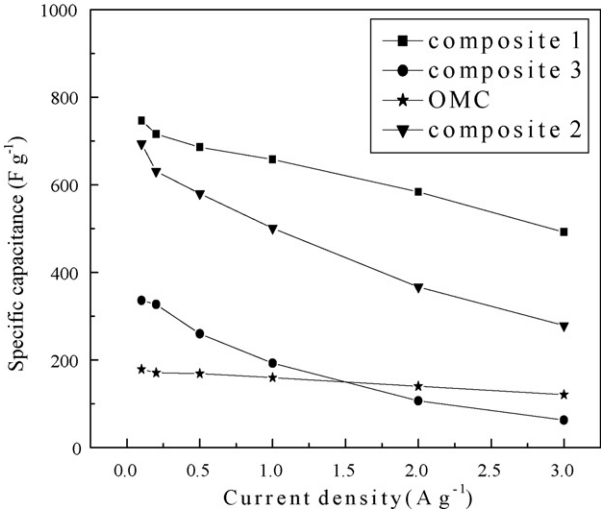

Fig. 6. The specific capacitances of OMC and three composites prepared via different methods at various current densities.

The calculated specific capacitances of OMC and three composites at different current densities are summarized in Fig. 6. It should be noted that at a current density of 0.1 A g^{-1} the specific capacitance (336 F g^{-1}) of composite 3 prepared via direct physical mixing method is not equal to the simple sum of that of PANI and OMC electrodes, and is higher than 179 F g^{-1} of pure OMC and 56 F g^{-1} of pure PANI. The result suggests that the simple introduction of OMC can also improve the electric contact between PANI and electrolyte to some extent and facilitate the faradaic charge-transfer, which is in agreement with the results of PANI/carbon nanotube composite [28,29]. Most importantly, the specific capacitances of composite 1 and composite 2 prepared via in situ polymerization method (747 and 694 F g^{-1}, respectively), are more than twice as high as those of composite 3, implying that the in-situ polymerization increases the degree of dispersion of PANI on carbon matrix, enhances the contact between PANI and OMC and allows electrolyte ions greater access to PANI. This makes more active sites of PANI available for faradic reaction and leads to the larger specific capacitance. Fig. 6 also displays the dependence of specific capacitance on current density in the range 0.1–3 A g^{-1}. The specific capacitance for all electrodes decreases with the increase of charge/discharge current density. However, at a current density of 3 A g^{-1} the specific capacitance of composite 1 is still as high as 492 F g^{-1}, which is about 66% of the specific capacitance at a current density of 0.1 A g^{-1}. The capacitance maintenance is near 68% of pure OMC and evidently higher than 40% of composite 2 and 21% of composite 3. This implies that composite 1 has the best rate capability among these materials. The results confirm that the double fixing effects of surface and mesopore of OMC on PANI make OMC a strong support, which benefits to the maintenance of electrical conductivity and mechanical strength of PANI and thus the improvement of rate performance of the material.

Cyclic voltammetry measurements were carried out within the potential range of 0.05–0.55 V to analyze the electrochemical behavior of the supercapacitors. Fig. 7A exhibits the cyclic voltammograms of composite 1 recorded at different sweep rates. Two obvious redox peaks are observed at about 0.48 and 0.35 V, respectively, which can be ascribed to the doping and dedoping of OH^- in the PANI composites. This resembles the behavior of PANI electrode in alkali (see Fig. 7B) or neutral aqueous solution [30]. The current clearly increases with sweep rate, indicating a good rate capability. The CV curves of all composites at a sweep rate of 10 mV s^{-1} are

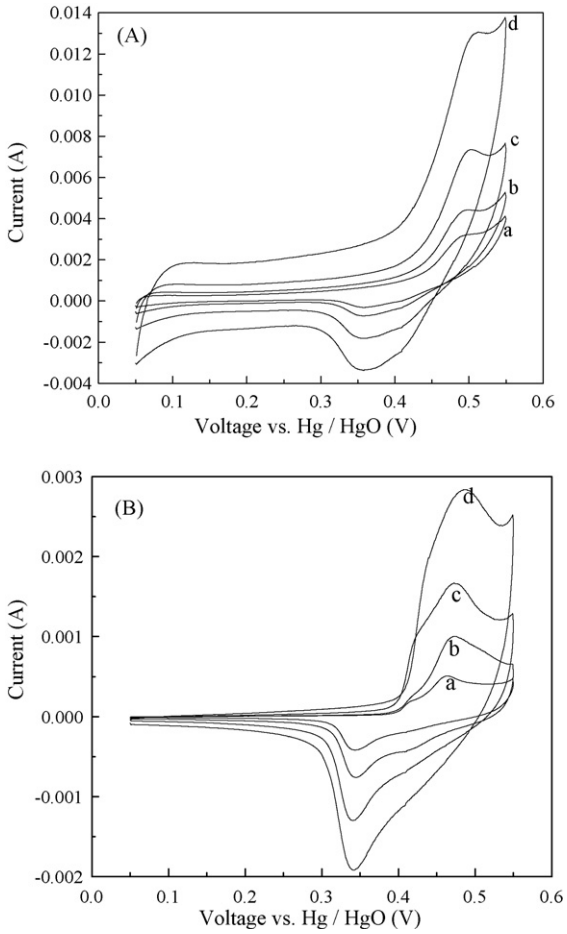

Fig. 7. Cyclic voltammograms of composite 1 (A) and PANI (B) electrodes at different sweep rates (a: 1 mV s^{-1}; b: 2 mV s^{-1}; c: 5 mV s^{-1}; d: 10 mV s^{-1}).

shown in Fig. 8. It is observed that under the same sweep rate the current of composite 1 in situ prepared using OMC as a starting material is higher than that of the other two. Therefore, its specific capacitance (according to the following relationship: the capacitance value equals the output current divided by the scan rate [31]) is the highest among them, which has probably resulted from the

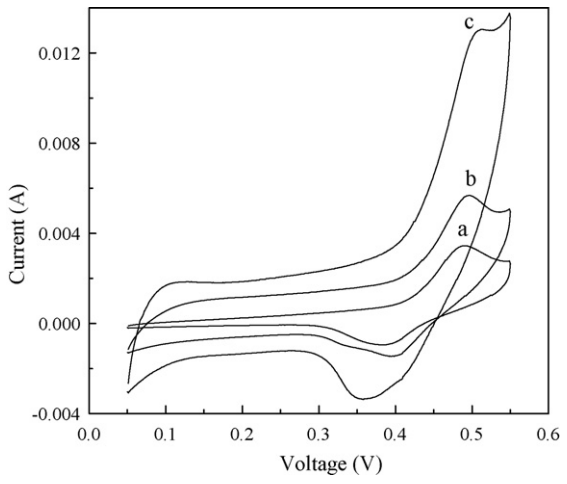

Fig. 8. Cyclic voltammograms of three composite electrodes (a: composite 3; b: composite 2; c: composite 1) at a sweep rate of 10 mV s^{-1}.

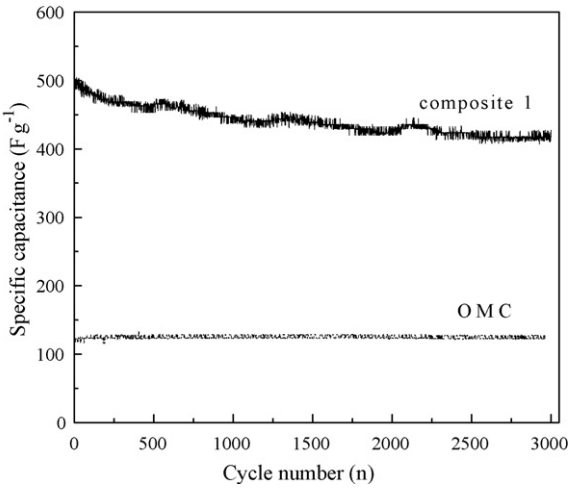

Fig. 9. Capacitance decaying curves of composite 1 and OMC electrodes.

double fixing effects of surface and mesopore of OMC upon PANI molecule. These results are in accordance with those deduced from the galvanostatic charge/discharge tests.

The cycling stability tests of OMC and composite 1 electrodes are investigated at a current density of 3 A g^{-1} and the results are shown in Fig. 9. For OMC electrode, the specific capacitance of 121 F g^{-1} is hardly changed during the charge/discharge cycling, indicating its stable cycle property. For composite 1 electrode, after 2000 times the specific capacitance stabilizes at 420 F g^{-1}, which is much higher than that of OMC. This exhibits the practical significance of composite 1 electrode. In addition, during the first 1000 cycles a lose of 12% in the specific capacitance value is observed, indicating that the research on improving stability electrochemical activity of PANI by the enhancement of interactions of PANI and OMC and control of configuration of PANI still needs to go on.

Electrochemical impedance spectroscopy (EIS) was further employed to monitor the electrochemical behavior of the electrodes. Typical Nyquist diagrams for OMC and composite 1 electrodes are given in Fig. 10. Two impedance curves show a single semicircle in the high frequency region and a sloped line in the low frequency region. Furthermore, it is clearly seen that composite 1

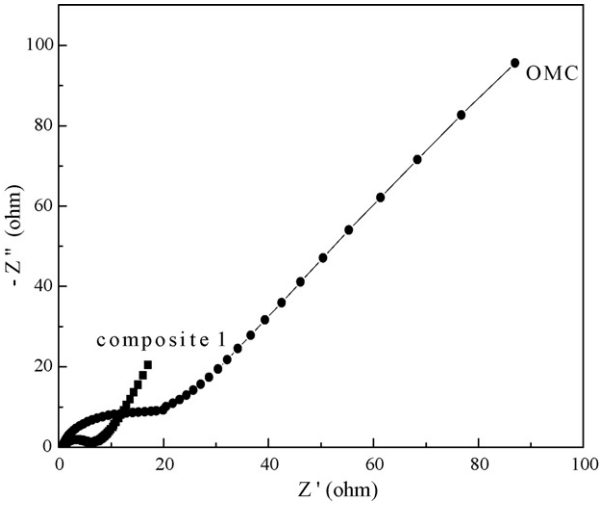

Fig. 10. Nyquist diagrams measured at 0.3 V applied potential for OMC and composite 1 electrodes.

induced a semicircle with smaller diameter than OMC, indicating its lower impedance on electrode/electrolyte interface.

4. Conclusions

In summary, three OMC/PANI composites were synthesized by different compounding processes, namely the in situ polymerization of aniline in the presence of OMC or its precursor (carbon/silica composite) and the direct physical mixing of PANI and OMC. Their supercapacitor behaviors in alkaline electrolyte were tested in detail by galvanostatic charge/discharge, cyclic voltammetry and AC impedance spectroscopy and the interaction mechanism of OMC and PANI was investigated by the analysis of their morphologies and structures. It has been found that whatever the compounding process was, the specific capacitances of the composites consisted of electric double-layer capacitance and faradaic capacitance. Moreover, the composite 1 prepared by using OMC as a starting material possesses not only a high specific capacitance of 747 F g^{-1} but also a good rate capability. The reason can be ascribed to the high degree of dispersion of PANI molecules and double fixing effects of the surface and mesopore of OMC on PANI, which made more PANI molecules available for faradaic reaction and OMC a stronger support for the maintenance of electrical conductivity and mechanical strength of PANI.

Acknowledgements

This work was supported by the Research Program of China Petrochemical Corporation (X504014), National Natural Science Foundation of China (50872006) and the Program for New Century Excellent Talents in University of China (NCET-04-0122).

References

[1] J.M. Ko, R.Y. Song, H.J. Yu, J.W. Yoon, B.G. Min, D.W. Kim, Electrochim. Acta 50 (2004) 873.
[2] R. Ryoo, S.H. Joo, S. Jun, J. Phys. Chem. B 103 (1999) 7743.
[3] J. Lee, S. Yoon, T. Hyeon, S.M. Oh, K.B. Kim, Chem. Commun. 21 (1999) 2177.
[4] S. Álvarez, M.C. Blanco-López, A.J. Miranda-Ordieres, A.B. Fuertes, T.A. Centeno, Carbon 43 (2005) 866.
[5] D. Wang, F. Li, M. Liu, H. Cheng, New Carbon Mater. 22 (2007) 307.
[6] L. Li, H. Song, X. Chen, Electrochim. Acta 51 (2006) 5715.
[7] W. Sugimoto, H. Iwata, Y. Yasunaga, Y. Murakami, Y. Takasu, Angew. Chem. Int. Ed. 42 (2003) 4092.
[8] V. Gupta, N. Miura, Electrochim. Acta 47 (2002) 4055.
[9] B.Y. Choi, I.J. Chung, J.H. Chun, J.M. Ko, Synth. Met. 99 (1999) 253.
[10] J.H. Park, J.M. Ko, O.O. Park, D.W. Kim, J. Power Sources 105 (2002) 20.
[11] K.M. Kim, N.G. Park, K.S. Ryu, S.H. Chang, Polymer 43 (2002) 3951.
[12] B. Fang, L. Binder, J. Electroanal. Chem. 609 (2007) 99.
[13] J.H. Park, O.O. Park, K.H. Shin, C.S. Jin, J.H. Kim, Electrochem. Solid State Lett. 5 (2002) H7.
[14] W. Chen, T. Wen, J. Power Sources 117 (2003) 273.
[15] J. Jang, J. Bae, M. Choi, S. Yoon, Carbon 43 (2005) 2730.
[16] V. Gupta, N. Miura, Electrochim. Acta 52 (2006) 1721.
[17] Y. Wang, H. Li, Y. Xia, Adv. Mater. 18 (2006) 2619.
[18] J. Kim, J. Lee, T. Hyeon, Carbon 42 (2004) 2711.
[19] D. Qu, H. Shi, J. Power Sources 74 (1998) 99.
[20] G.V. Ramana Reddy, C. Ramesh Kumar, R. Sriram, J. Appl. Polym. Sci. 94 (2004) 739.
[21] M.R. Karim, C.J. Lee, M.S. Lee, J. Appl. Polym. Sci. 103 (2006) 1973.
[22] H.K. Chaudhari, D.S. Kelkar, Polym. Int. 42 (1997) 380.
[23] S. Virji, R.B. Kaner, B.H. Weiller, Chem. Mater. 17 (2005) 1256.
[24] M. Kruk, M. Jaroniec, Chem. Mater. 13 (2001) 3169.
[25] Y. Zheng, M. Zhang, P. Gao, Mater. Res. Bull. 42 (2007) 1740.
[26] E. Frackowiak, V. Khomenko, K. Jurewicz, K. Lota, F. Béguin, J. Power Sources 153 (2006) 413.
[27] A.K. Shukla, S. Sampath, K. Vijayamohanan, Curr. Sci. 79 (2000) 1656.
[28] Y. Zhou, B. He, W. Zhou, J. Huang, X. Li, B. Wu, H. Li, Electrochim. Acta 49 (2004) 257.
[29] B. Dong, B. He, C. Xu, H. Li, Mater. Sci. Eng. B 143 (2007) 7.
[30] J.H. Park, O.O. Park, J. Power Sources 111 (2002) 185.
[31] J. Wang, Y. Xu, X. Chen, X. Du, J. Power Sources 163 (2007) 1120.